Int. J. Electrochem. Sci., 5 (**2010**) 56 - 71

International Journal of
ELECTROCHEMICAL
SCIENCE
www.electrochemsci.org

Corrosion of Aged and Annealed 18 Ni 250 Grade Maraging Steel in Phosphoric Acid Medium

T. Poornima[1], *Jagannath Nayak*[2] *and A. Nityananda Shetty*[3,*]

[1] Department of Science and Humanities, PESIT Bangalore-560085, India
[2] Department of Metallurgical and Materials Engineering, National Institute of Technology Karnataka, Surathkal, Post Srinivasnagar, Mangalore-575025 Karnataka, India
[3] Department of Chemistry, National Institute of Technology Karnataka, Surathkal, Post Srinivasnagar, Mangalore-575025 Karnataka, India
[*]E-mail: nityashreya@gmail.com

Received: 28 November 2009 / *Accepted:* 11 January 2010 / *Published:* 31 January 2010

The corrosion behavior of aged and annealed sample of 18 Ni 250 grade maraging steel was investigated in phosphoric acid over a range of acid concentration and solution temperature by using electrochemical techniques like Tafel extrapolation and electrochemical impedance spectroscopy. The studies have revealed that the corrosion rate of both aged and annealed samples increase with increase in temperature and increase in concentration of phosphoric acid in the medium. The corrosion rate of annealed sample is found to be less than that of aged sample. The thermodynamic parameters like activation energy, enthalpy of activation and entropy of activation for the corrosion process were calculated.

Keywords: Maraging Steel, Acid solutions, EIS, Polarisation

1. INTRODUCTION

Corrosion of structural elements is a major issue for any industry because of the chemical environment of chemical processing. Maraging steels are special class of ultra high strength steels that differ from conventional steels in that they are hardened by a metallurgical reaction that does not involve carbon [1]. They derive high strength from age hardening of low carbon, Fe-Ni martensitic matrix [2]. Recently, the needs of high reliable substances of high strength and high ductility are gradually increased with the development of aerospace industry. The characteristics of this grey and white steel are high ductility, formability, high corrosion resistance, high temperature strength, ease of fabrication, weldability and maintenance of an invariable size even after heat treatment [3]. According to available literature, atmospheric exposure of 18 Ni maraging steel leads to corrosion in a uniform manner and become completely rust covered [4]. Pit depths tend to be shallower than high strength steels [5]. Bellanger et al [6] have studied the effect of slightly acid pH with or without chloride in radioactive water on the corrosion of maraging steel and have reported that corrosion behavior of maraging steel at the corrosion potential depends on pH, and intermediates remaining on maraging steel surface in the active region favoring the passivity. The effect of carbonate ions in slightly alkaline medium on the corrosion of maraging steel was studied by Bellanger [7]. The corrosion rate of maraging steel in acid solutions such as sulphuric acid, hydrochloric acid, formic acid, and stearic acid are substantial. Heat treatment affects the corrosion rate. Critical and passive current densities increase as the structure is varied from fully annealed to fully aged [8]. Maraging steels are found to be less susceptible to hydrogen embrittlement than common high strength steels owing to significantly low diffusion of hydrogen in them [9]. Several technical papers covering alloy design, material processing, thermo-mechanical treatments, welding, strengthening mechanisms, etc., have been published [10]. These steels have emerged as alternative materials to conventional quenched and tempered steels for advanced technologies such as aerospace, nuclear and gas turbine applications. They frequently come in contact with acids during cleaning, pickling, descaling, acidising, etc. Most of the reported studies were conducted on corrosion of various metals and alloys in HCl and H_2SO_4 medium. Phosphoric acid is also used in pickling delicate, costly components and precision items where rerusting after pickling has to be avoided. Muralidaran et al [11] reported the reduction in corrosion rate of iron in phosphoric acid with immersion time and they attributed this due to surface coverage by phosphate. Materials used in acid environment should have good corrosion resistance. The stress corrosion cracking behavior and also hydrogen embrittlement in these steels have been studied quite extensively. But no literature seems to be available which reveal corrosion behavior of 18 Ni 250 grade maraging steel in acid medium. So it is intended to study the corrosion behavior of maraging steel in phosphoric acid medium.

2. EXPERIMENTAL PART

2.1. Material

The maraging steel samples (M 250 grade) in annealed and aged condition were taken from plates which were subjected to solution annealing treatment at 815 ± 5^{o}C for 1 hour followed by air cooling. Percentage composition of 18 Ni 250 grade maraging steel samples in annealed and aged condition is given in Table 1. Cylindrical test coupons were cut from the plate and sealed with epoxy resin in such a way that, the area exposed to the medium is 0.503 cm^2. These coupons were polished as per standard metallographic practice, belt grinding followed by polishing on emery papers, finally on polishing wheel using legated alumina to obtain mirror finish, degreased with acetone, washed with double distilled water and dried before immersing in the corrosion medium.

Table 1. Composition of the specimen (% by weight)

Element	Composition	Element	Composition
C	0.015%	Ti	0.3-0.6%
Ni	17-19%	Al	0.005-0.15%
Mo	4.6-5.2%	Mn	0.1%
Co	7-8.5%	P	0.01%
Si	0.1%	S	0.01%
O	30 ppm	N	30 ppm
H	2.0 ppm	Fe	Balance

2.2. Medium

Standard solutions of phosphoric acid having concentration 0.02 M, 0.04 M, 0.2 M, 0.4 M, 0.6 M and 0.8 M (corresponding H^+ ion concentrations, 0.06 M, 0.12 M, 0.6 M, 1.2 M, 1.8 M and 2.4 M, respectively) were prepared by diluting analytical grade (Nice) phosphoric acid with double distilled water. Experiments were carried out using calibrated thermostat at temperatures 30 °C, 35 °C, 40 °C, 45 °C, 50 °C (±0.5 °C)

2.3. Electrochemical measurements

2.3.1. Tafel polarisation studies

Electrochemical measurements were carried out by using an electrochemical work station, Auto Lab 30 and GPES software. Tafel plot measurements were carried out using conventional three electrode Pyrex glass cell with platinum counter electrode and saturated calomel electrode as reference electrode. All the values of potential are therefore referred to the SCE. Finely polished annealed and aged maraging steel specimens of 0.503 cm^2 surface area were exposed to corrosion medium of different concentrations of phosphoric acid (0.02 M to 0.8 M) at different temperatures (30 °C to 50 °C) and allowed to establish a steady state open circuit potential. The potentiodynamic current-potential curves were recorded by polarising the specimen to -250 mV cathodically and +250 mV anodically with respect to open circuit potential (OCP) at scan rate of 5 $mV\ s^{-1}$.

2.3.2. Electrochemical impedance spectroscopy studies (EIS)

Electrochemical impedance spectroscopy (EIS), which gives early information about the electrochemical processes, at the metal solution interface, has been used in many reports on the corrosion studies [12]. The corrosion behavior of the specimen in annealed and aged condition was also obtained from EIS technique using electrochemical work station, Auto Lab 30 and FRA software. In EIS technique a small amplitude ac signal of 10 mV and frequency spectrum from 100 kHz to 0.01 Hz was impressed at the OCP and impedance data were analyzed using Nyquist plots. The charge transfer resistance, R_t was extracted from the diameter of the semicircle in Nyquist plot..

In all the above measurements, at least three similar results were considered and their average values are reported.

The scanning electron microscope images were recorded to establish the interaction of acid medium with the metal surface using JEOL JSM-6380LA analytical scanning electron microscope.

3. RESULTS AND DISCUSSION

3.1. Tafel polarisation measurement

The effect of phosphoric acid concentration and solution temperature on the corrosion rate of annealed and aged samples of maraging steel was studied using Tafel polarisation technique. Fig 1 and Fig 2 represent potentiodynamic polarisation curves of annealed and aged samples of maraging steel respectively as a function of concentration of phosphoric acid at 30° C. The corrosion current densities (i_{corr}) obtained by the Tafel extrapolation technique increases with increase in concentration of phosphoric acid in the solution for both the samples.

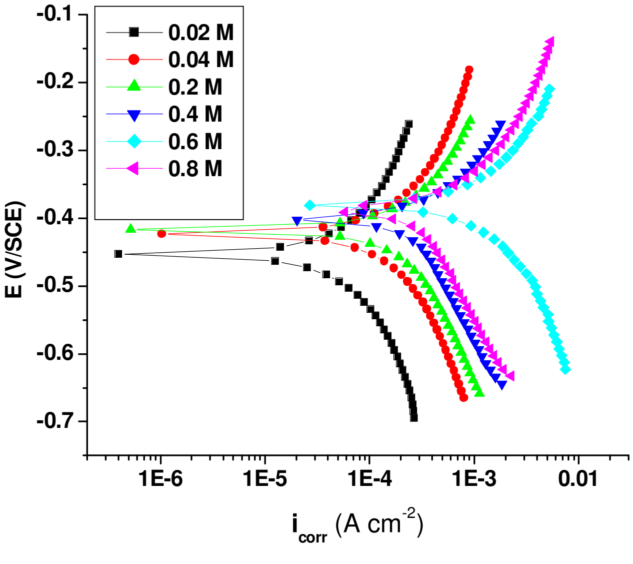

Figure 1. Potentiodynamic polarisation curves of annealed maraging steel specimen in different concentrations of H_3PO_4 at 30^0C

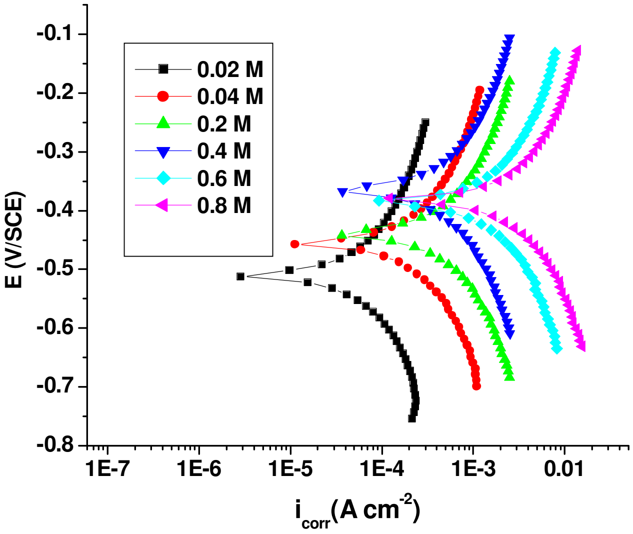

Figure 2. Potentiodynamic polarisation curves of aged maraging steel specimen in different concentrations of H_3PO_4 at 30^0C

Fig 3 and Fig 4 represent potentiodynamic polarisation curves of annealed and aged maraging steel specimen, respectively, in phosphoric acid as a function of temperature. The corrosion current densities (i_{corr}) obtained by the Tafel extrapolation technique increases with increase in temperature of the acid solution for both the samples.

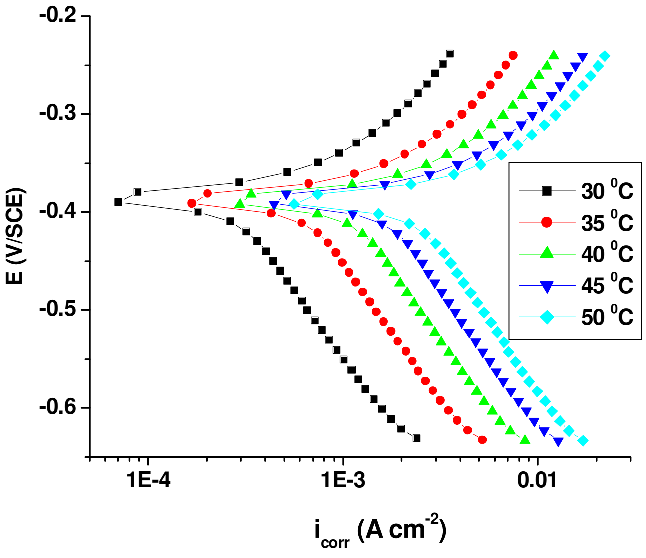

Figure 3. Potentiodynamic polaristion curves of annealed maraging steel specimen at different temperatures in 0.6 M phosphoric acid

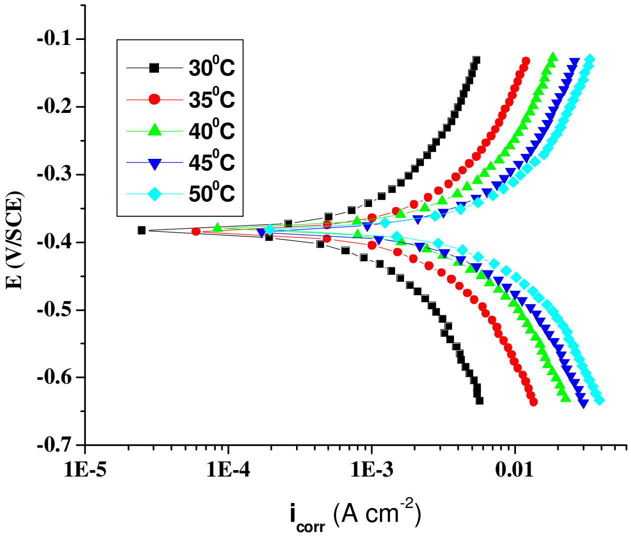

Figure 4. Potentiodynamic polaristion curves of aged maraging steel specimen at different temperatures in 0.6 M phosphoric acid

The potentiodynamic polarisation parameters like corrosion potential (E_{corr}), corrosion current (i_{corr}), polarisation resistance (R_p), anodic and cathodic slopes (b_a and b_c), and corrosion rate are calculated from Tafel plots and are tabulated in Table 2 and Table 3 for annealed and aged samples respectively.

These results indicate that with increase of both concentration of phosphoric acid and solution temperature the R_p value decreases, polarisation curves are shifted to high current density region indicating increase in corrosion rate. The nature of polarisation curves predicts active corrosion behavior at each temperature and concentration of phosphoric acid. It is observed from these results that the corrosion potential is shifted to noble values as the concentration of phosphoric acid is increased. This is in accordance with Murralidharan et al [11] who proposed dependence of E_{corr} and I_{corr} on solution parameters. The positive shift in the corrosion potential, E_{corr}, indicates that the anodic process is much more affected than the cathodic [13]. With increase of solution temperature b_a and b_c are almost unchanged indicating no change in the mechanism of corrosion with temperature. The increasing corrosion rate with increasing temperature is in agreement with the observation reported by Jones that, in open system, the corrosion rate of iron increases with temperature up to 80 °C [14]. This can also be explained by the characteristics of the cathodic process of hydrogen evolution in acidic solutions. The hydrogen evolution overpotential decreases with increase in temperature that leads to increase in cathodic reaction rate [15]. The corrosion rate reaches a maximum value of 17.3 mm y^{-1} for annealed specimen and 23 mm y^{-1} for aged specimen in 0.8 M phosphoric acid at 50 °C.

Table 2. Results of Tafel polarization and the electrochemical impedance studies for the annealed specimen.

Molarity of H_3PO_4	Tafel polarization results							EIS results
	T (K)	E_{corr} (V vs SCE)	R_p (ohm cm^2)	i_{corr} (x 10^{-4} A cm^{-2})	$-b_c$ (V dec^{-1})	b_a (V dec^{-1})	Corrosion rate (mm y^{-1})	R_t (ohm cm^2)
0.02	303	-0.423	137.8	01.13	0.107	0.099	1.01	102.1
	308	-0.426	134.3	01.22	0.123	0.112	1.23	99.6
	313	-0.429	117.2	01.50	0.111	0.122	1.44	95.6
	318	-0.433	112.2	01.62	0.106	0.134	1.61	91.5
	323	-0.429	109.2	01.72	0.121	0.123	1.93	89.5
0.04	303	-0.417	96.6	01.83	0.137	0.108	2.13	65.4
	308	-0.417	89.0	02.14	0.151	0.118	2.49	59.9
	313	-0.418	85.0	02.66	0.132	0.131	2.83	54.3
	318	-0.419	77.5	02.99	0.135	0.126	3.30	49.3
	323	-0.423	66.4	03.75	0.136	0.123	3.69	45.3
0.2	303	-0.400	48.8	02.79	0.119	0.084	3.25	37.2
	308	-0.400	39.7	03.73	0.161	0.078	4.33	30.7
	313	-0.400	33.7	04.70	0.152	0.088	5.46	27.2
	318	-0.401	31.7	05.57	0.177	0.090	6.53	22.1
	323	-0.403	28.2	06.27	0.170	0.092	7.37	18.1
0.4	303	-0.396	34.7	04.57	0.245	0.079	5.30	27.2
	308	-0.391	31.2	05.81	0.266	0.083	6.74	23.6
	313	-0.392	25.2	07.12	0.275	0.092	8.26	22.1
	318	-0.392	22.6	08.43	0.259	0.095	9.76	20.1
	323	-0.394	19.6	09.79	0.256	0.098	11.34	18.6
0.6	303	-0.384	31.2	05.14	0.278	0.064	5.93	29.2
	308	-0.386	24.6	07.01	0.298	0.104	8.14	24.7
	313	-0.386	20.6	08.55	0.302	0.084	10.08	18.6
	318	-0.386	17.6	09.92	0.306	0.075	11.98	17.1
	323	-0.388	16.6	11.24	0.274	0.082	14.02	16.1
0.8	303	-0.378	26.7	6.22	0.271	0.085	7.23	26.2
	308	-0.380	21.6	9.34	0.275	0.099	9.53	19.6
	313	-0.380	18.1	11.8	0.313	0.093	12.63	18.1
	318	-0.380	14.6	14.6	0.226	0.073	15.13	13.6
	323	-0.382	12.6	16.8	0.256	0.090	17.32	12.1

Table 3. Results of Tafel polarization and the electrochemical impedance studies for the aged specimen

Molarity of H_3PO_4		Tafel polarization results						EIS results
	T (K)	E_{corr} (V vs SCE)	R_p (ohm cm^2)	i_{corr} (x 10^{-4}) (A cm^{-2})	$-b_c$ (V dec^{-1})	b_a (V dec^{-1})	Corrosion rate (mm y^{-1})	R_t (ohm cm^2)
0.02	303	-0.456	115.7	1.676	0.087	0.082	2.03	104.6
	308	-0.456	106.1	1.908	0.103	0.090	2.25	90.5
	313	-0.462	90.0	1.991	0.090	0.096	2.48	82.5
	318	-0.454	73.9	2.303	0.100	0.102	2.67	76.5
	323	-0.470	66.9	2.542	0.086	0.107	2.86	70.9
0.04	303	-0.438	95.6	1.925	0.080	0.084	2.44	98.1
	308	-0.445	73.4	2.643	0.083	0.092	2.89	89.5
	313	-0.436	71.9	2.962	0.087	0.090	3.06	78.5
	318	-0.454	66.4	3.03	0.100	0.102	3.47	68.9
	323	-0.439	59.9	3.623	0.099	0.097	3.91	61.4
0.2	303	-0.400	35.7	4.816	0.084	0.105	5.06	29.2
	308	-0.401	31.7	5.723	0.085	0.104	5.58	22.6
	313	-0.400	28.7	6.150	0.095	0.097	6.38	18.6
	318	-0.397	27.7	6.699	0.108	0.110	6.89	15.1
	323	-0.395	26.2	7.507	0.100	0.130	7.39	14.1
0.4	303	-0.384	22.1	8.263	0.123	0.118	8.49	19.6
	308	-0.383	18.6	9.441	0.098	0.174	9.53	15.6
	313	-0.380	18.6	10.345	0.095	0.170	10.68	13.6
	318	-0.379	18.1	11.441	0.110	0.119	11.79	12.1
	323	-0.380	14.6	12.84	0.096	0.115	13.08	9.6
0.6	303	-0.379	26.1	11.074	0.100	0.106	11.23	7.1
	308	-0.375	24.6	12.50	0.106	0.115	12.81	6.5
	313	-0.375	21.1	14.26	0.104	0.099	14.40	6.0
	318	-0.371	18.1	15.53	0.105	0.097	15.94	5.0
	323	-0.375	15.1	16.89	0.122	0.099	17.52	4.5
0.8	303	-0.368	14.1	13.23	0.100	0.117	13.84	6.5
	308	-0.371	12.6	15.84	0.095	0.111	16.02	6.0
	313	-0.371	12.1	17.86	0.107	0.107	18.29	5.0
	318	-0.363	11.1	19.61	0.100	0.132	19.97	4.5
	323	-0.371	10.3	22.45	0.134	0.110	22.48	4.0

At the interface of iron and acid electrolyte, the dissolution of iron can be written as follows[16]:

$$Fe + H_2O \Leftrightarrow FeOH_{ads} + H^+ + e^- \quad (1)$$
$$FeOH_{ads} \rightarrow FeOH^+ + e^- \quad (2)$$
$$FeOH^+ \Leftrightarrow Fe^{2+} + OH^- \quad (3)$$

At medium and high concentrations of phosphoric acid, precipitation of iron phosphate occurs at the interface [17] as follows:

$$6H_3PO_4 + 3Fe \rightarrow 3Fe(H_2PO_4)_2 + 3H_2 \quad (4)$$
$$3Fe(H_2PO_4)_2 \rightarrow Fe_3(PO_4)_2 + 4H_3PO_4 \quad (5)$$

It is observed that corrosion rate follows Arrhenius law equation 6.

$$\ln k = B - (E_a/RT) \quad (6)$$

where k is the rate constant, B is a constant which depends on the metal type, E_a is the activation energy, T is the temperature in K and R is the universal gas constant. The plot of ln(corrosion rate) vs reciprocal of absolute temperature (1/T) gives straight line with slope = $-E_a/R$. The Arrhenius plots, ln(corrosion rate) vs reciprocal of absolute temperature 1/T, for the annealed and aged specimens are shown in Fig 5 and Fig 6, respectively. From the slopes of the plots activation energy for the corrosion process was calculated and they are given in table 4. The activation energy values obtained for the annealed specimen indicate that the whole process is controlled by surface reaction, since the values of energy of activation for corrosion process are greater than 20 kJ mol^{-1} [18]. Approximately similar values of E_a were obtained at different concentrations of acid. This phenomenon may be due to the fact that the activation energy for the corrosion reaction is independent of acid concentration [19].

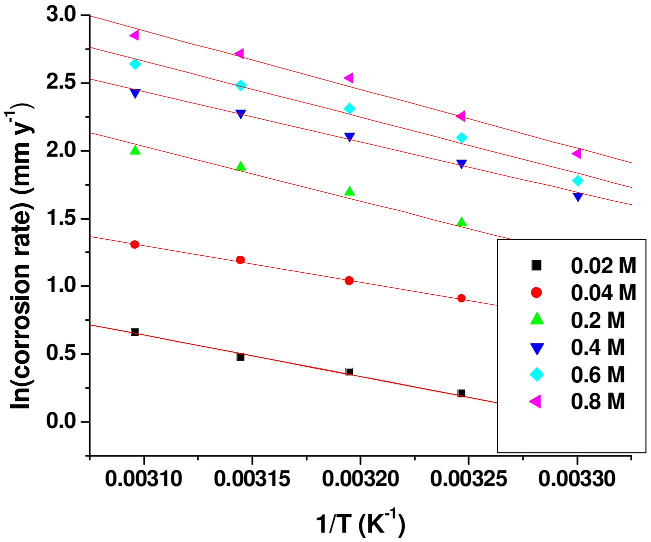

Figure 5. Arrhenius plots for annealed sample of maraging steel in H_3PO_4

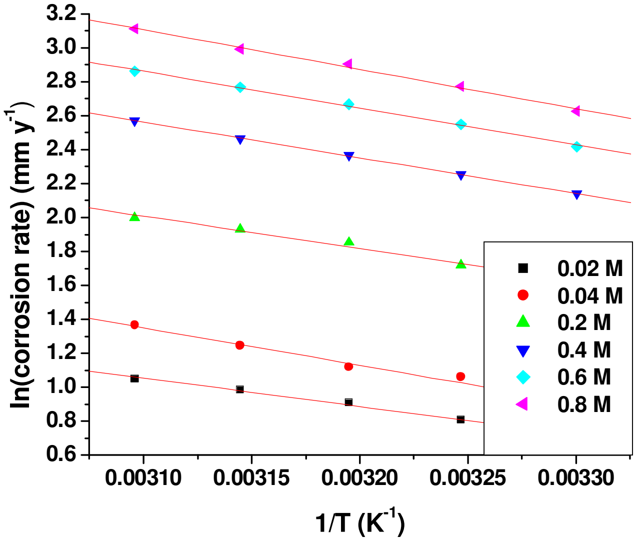

Figure 6. Arrhenious plots for aged sample of maraging steel in H_3PO_4

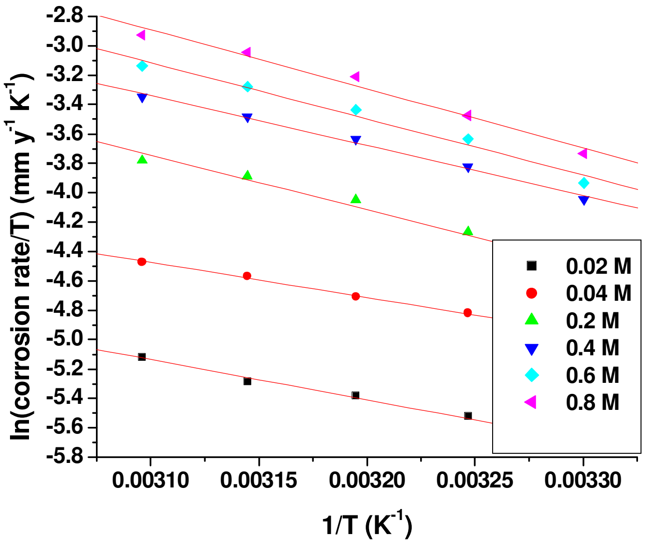

Figure 7. ln(corrosion rate/T) vs 1/T for annealed sample of maraging steel in H_3PO_4

Entropy and enthalpy of activation ($\Delta H^{\#}$ & $\Delta S^{\#}$) were calculated from transition state theory equation 7 and these values are given Table 4.

$$k = (RT/Nh)\exp(\Delta S^{\#}/R)\exp(-\Delta H^{\#}/RT) \qquad (7)$$

where h is Plank's constant, N is Avagadro's number. A plot of ln(corrosion rate/T) vs 1/T gives straight line with slope = $-\Delta H^{\#}/R$ and intercept = $\ln(R/Nh) + \Delta S^{\#}/R$. Fig. 7 and Fig.8 give the plot of ln(corrosion rate/T) vs 1/T for annealed and aged samples of maraging steel, respectively, in various concentrations of phosphoric acid. The entropy of activation is large and negative. This implies that the activated complex in the rate determining step represents association rather than dissociation, indicating that a decrease in disorder takes place, in going from reactant to the activated complex [20]. The value of $\Delta S^{\#}$ increases with increase in acid concentration reveals that dissolution of alloy is facilitated as the concentration of the acid medium increases.

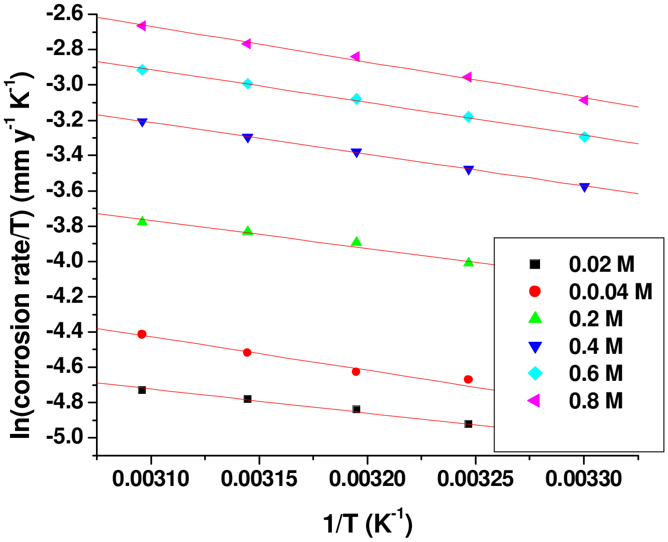

Figure 8. ln(corrosion rate/T) vs 1/T for aged sample of maraging steel in phosphoric acid

Table 4. Activation parameters of corrosion reaction of annealed and aged specimens in phosphoric acid

Molarity of H_3PO_4	E_a (kJ mol^{-1})		$\Delta H^{\#}$ (kJ mol^{-1})		$\Delta S^{\#}$ (J mol^{-1} K^{-1})	
	Annealed	Aged	Annealed	Aged	Annealed	Aged
0.02	25.37	13.93	22.78	11.33	-169.70	-201.72
0.04	22.50	18.42	19.90	15.82	-173.10	-185.33
0.2	33.45	15.80	30.86	13.20	-133.10	-187.9
0.4	30.81	17.53	28.21	14.93	-137.90	-177.99
0.6	34.38	18.05	31.78	15.45	-124.90	-173.89
0.8	36.02	19.40	33.43	16.80	-118.00	-167.69

From the results of Tafel polarisation and activation energy values we can observe that the corrosion rate of annealed sample is less than that of aged samples in phosphoric acid. This may be attributed to the fact that annealed samples are solution treated and air cooled. These samples contain entirely martensitic matrix which is composed of predominantly iron and nickel. Hence corrosion behavior of annealed samples is similar to that of iron and nickel in acid medium. Aging results in precipitation of intermetallics. Since these intermetallics have different composition, their electrochemical behavior is expected to be different compared to matrix [21]. Also there will be strain fields around these coherent precipitates as a result of lattice mismatch between the precipitate and the matrix due to the difference in the crystal structure and lattice parameters. These strain fields in combination with the galvanic effect due to the composition difference leads to the enhanced corrosion of aged samples than the annealed samples.

3.2. Electrochemical impedance spectroscopy

The corrosion behavior of annealed and aged samples of maraging steel specimens was also investigated by EIS in various concentrations of phosphoric acid at various temperatures. The impedance spectra recorded are displayed as Nyquists plots for annealed specimen as a function of concentration of acid and temperature as shown in Fig 9 and Fig 10, respectively. Similar plots were obtained for aged specimen also which are not given here.

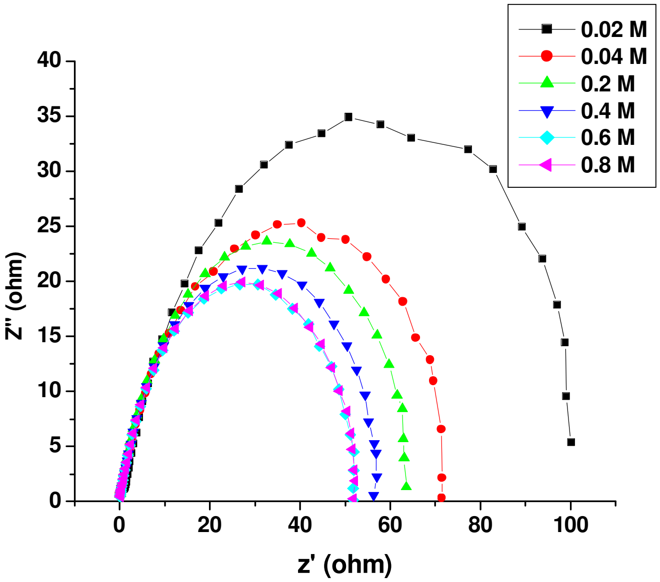

Figure 9. Nyquist plots for annealed maraging steel specimen in various concentrations of H_3PO_4

The depressed semicircles of the Nyquist plots suggest the distribution of capacitance due to inhomogeneities associated with the electrode surface [22]. In order to analyse the impedance spectra containing one capacitive loop, the equivalent circuit given in Fig 11 is used, which has been used previously to model iron/acid interface [23]. The capacitive loops are not perfect semicircles, because the Nyquist plots obtained in the real system represent a general behavior where the double layer at the metal solution interface does not behave as an ideal capacitor [24,25]. The fact that impedance diagrams have a semicircular appearance shows that the corrosion of steel is controlled by charge transfer process [26,27]. The intersection of capacitive loop with the real axis on the high frequency region represents the ohmic resistances of corrosion product films and the solution enclosed between the working electrode and the reference electrode, R_s. R_t represents the charge transfer resistance whose value is a measure of electron transfer across the surface and is inversely proportional to corrosion rate [28]. In evaluation of Nyquists plot, the difference in real impedance at lower and higher frequencies is considered as charge transfer resistance R_t [29]. The diameter of the semicircle decreases as acid concentration and solution temperature increases indicating increase in corrosion rate.

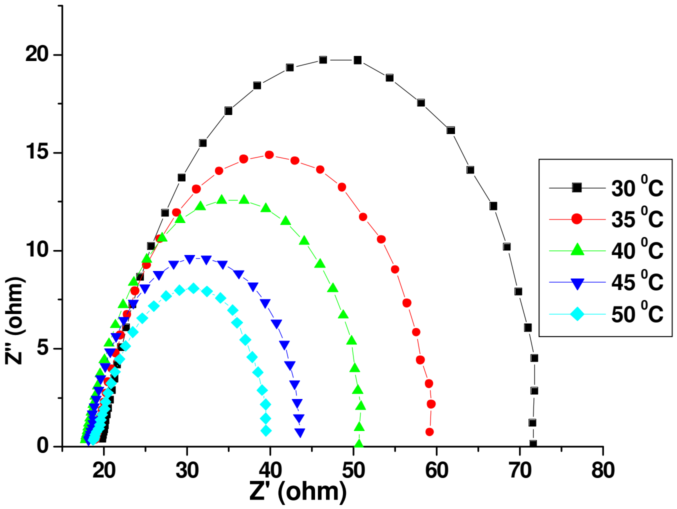

Figure 10. Nyquist plots for annealed maraging steel specimen in 0.6 M phosphoric acid at different temperatures.

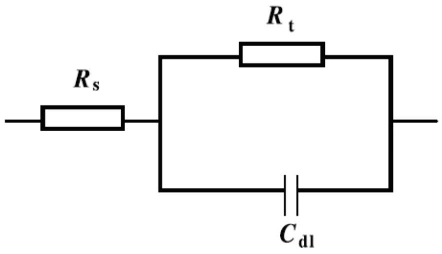

Figure 11. Equivalent circuit for the metal/acid interface. (R_s solution resistance, R_t charge transfer resistance, C_{dl} double layer capacitance.)

The corrosion current density I_{corr} is related to charge transfer resistance R_t, by Stern- Geary equation[13,20].

$$I_{corr} = \frac{b_a b_c}{2.303 R_t A (b_a + b_c)} \tag{8}$$

where R_t is charge transfer resistance obtained from Nyquists plots. A is area of cross section of material under observation b_a and b_c are Tafel constants.

The R_t values obtained from Nyquist plots for both annealed and aged samples of maraging steel at various acid concentrations and solution temperatures are summarized in Table 2 and Table 3. The results obtained by EIS method at various concentrations of acid and solution temperature are similar to that of Tafel polarization results.

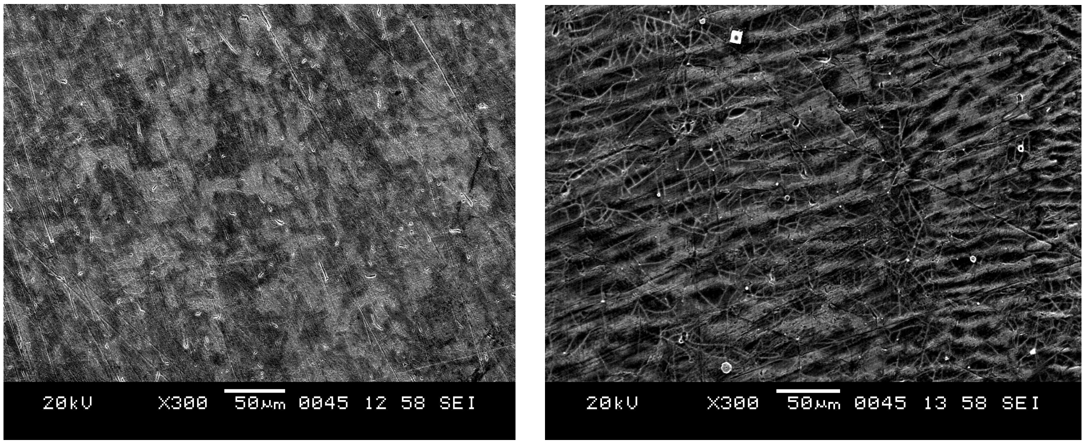

(a) (b)

Figure 12. SEM images of annealed specimen. (a). Freshly polished surface (b). Corroded surface after polarisation experiment in H_3PO_4

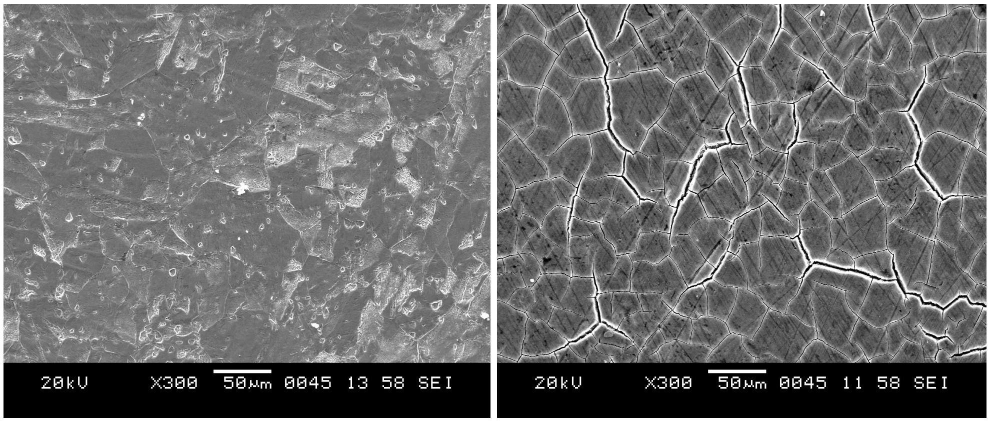

(a) (b)

Figure 13. SEM images of the aged specimen. a). Freshly polished surface b). Corroded surface polarisation experiment in H_3PO_4.

3.3. Scanning electron microscope studies (SEM)

The SEM images of freshly polished surface of annealed and aged samples of maraging steel are given in Figures 12a and 13a which show uncorroded surface with few scratches due to polishing. The surface morphology of the annealed and aged samples was examined by SEM immediately after corrosion tests in phosphoric acid medium. The SEM image of corroded annealed sample in Fig 12b shows degradation of alloy, with more or less uniform attack. In the case of corroded aged samples this degradation is highly pronounced as shown in Fig 13b, seems to be concentrated more on and around the grain boundaries. The intermetallic precipitation at grain boundary may be responsible for the higher rate of corrosion.

4. CONCLUSIONS

Based on results of investigation, the following conclusions may be drawn.

1. The corrosion rate of annealed and aged maraging steel specimen in phosphoric acid medium is substantial.
2. The corrosion rates of both the specimens are influenced by temperature and concentration of phosphoric acid medium. The corrosion rate of both the specimens under investigation increases with increase in concentration of phosphoric acid and solution temperature.
3. The corrosion kinetics follows Arrhenius law.
4. The corrosion rate of annealed sample is less than that of aged sample in phosphoric acid medium.

References

1. K. Y. Sastry, R. Narayanan, C. R. Shamantha, S. S. Sunderason, S. K. Seshadri SK, V. M. Radhakrishnan, K. J. L. Iyer, S. Sundararajan, *Mat. Sci. and Techn.,* 19 (2003) 375.
2. ASM Hand Book (1990) vol.1, 10th ed, ASM International
3. D. G. Lee, K. C. Jang, J. M. Kuk, I. S. Kim, *J. of Mat. Proc. Techn.,* 162 (2005) 342.
4. W. W. Krick, R. A. Covert, T. P. May, *Met. Eng. Quart.,* 8 (1968) 31
5. S. W. Dean, H. R. Copson, *Corrosion,* 21 (1965) 95.
6. G. Bellanger, J. J. Rameau, *J. Nuclear Mat.,* 228 (1996) 24.
7. G. Bellanger, *J.Nuclear Mat.,* 217 (1994) 187.
8. Data bulletin on 18%Ni maraging steel (1964), The International Nickel Company, INC.
9. J. Rezek, I. E. Klein, J. Yhalom, (1997) *Corros. Sci.,* 39 (1997) 385.
10. P. P. Sinha, *IIM Metal News* (1999) 2(5).
11. V. S. Muralidharan, K. S. Rajagopalan, *Corros. Sci.,* 19 (1979) 207.
12. Quartarone, M. Battilana, L. Bonaldo, T. Tortato, *Corros. Sci.,* 50 (2008) 3468.
13. A. El- Sayed, *J Appl. Electrochem.,* 27 (1997) 94.
14. F. N. Speller, *Corrosion causes and prevention,* 3rd edition, McGraw Hill, (1951)168
15. L. Larabi, Y. Harek, O. Benali, S. Ghalem, *Prog. Org. Coat.,* 54 (2005) 261
16. G. Gunasekaran, L. R. Chauhan, *Electrochim. Acta.,* 49 (2004) 4393

17. E. Almeida, D. Pereira, M.O. Figueiredo, V. M. M. Lobo, M. Morcillo, *Corros. Sci.,* 39 (1997) 1561
18. K. K. H. El-Neami, A. K. Mohamed, A. S. Kenawy IN Fouda, *Monatsh. Chem. J.,* 126 (1995) 369
19. M. S. Morad, *Mat. Chem. Phy.,* 60 (1999) 190
20. S. S. Abd Ei-Rehim, M. A. M. Ibrahim, K. F. Khaled, *J. Appl. Electrochem.*, 29 (1999) 593
21. D. W. Shoesmith, *Metals Handbook,* 9th ed. volume 13, 18
22. E. E. Oguzie, Y. Li, F. H. Wang, *Electrochim. Acta.,* 52 (2007) 6988
23. M. E. Azhar, B. Mernari, M. Traisnel, F. Bentiss, M. Lagrenee, *Corros. Sci.,* 43 (2001) 2229
24. Sha Cheng, Shougang Chen,Tao Liu, Xueting Chang, Yansheng Yin, *Electrochim. Acta.,* 52 (2007) 5932.
25. M. Ozcan, I. Dehri, M. Erbil, *Appl. Surf. Sci.,* 236 (2004) 155
26. L. Lrabi, Y. Harek, M. Traisnel, Mansri, *J. Appl. Electrochem.,* 34 (2004) 833
27. Qing Qu, Shuan Jiang, Wei Bai, Lei Li, *Electrochim. Acta.,* 52 (2007) 6811
28. H. H. Hamdy, A. Essam, A. A. Mohammed, *Electrochim. Acta.,* 52 (2007) 6359
29. M. Ozcan, I. Dehri, *Prog. Org. Coat.,* 51 (2004) 183.